

# Abductive Action Inference

Clement Tan<sup>1</sup>, Chai Kiat Yeo<sup>1</sup>, Cheston Tan<sup>2</sup>, Basura Fernando<sup>2</sup>

<sup>1</sup>Nanyang Technological University, Singapore

<sup>2</sup>Centre for Frontier AI Research (CFAR), Agency for Science, Technology and Research (A\*STAR),  
1 Fusionopolis Way, #16-16 Connexis, Singapore 138632, Republic of Singapore

{s190099, asckyeo}@e.ntu.edu.sg, {cheston-tan@i2r, fernando\_basura@ihpc}.a-star.edu.sg

## Abstract

Abductive reasoning aims to make the most likely inference for a given set of incomplete observations. In this work, we propose a new task called abductive action inference, in which given a situation, the model answers the question ‘what actions were executed by the human in order to arrive in the current state?’. Given a state, we investigate three abductive inference problems: action set prediction, action sequence prediction, and abductive action verification. We benchmark several SOTA models such as Transformers, Graph neural networks, CLIP, BLIP, end-to-end trained Slow-Fast, and Resnet50-3D models. Our newly proposed object-relational BiGED model outperforms all other methods on this challenging task on the Action Genome dataset. Codes will be made available.

## 1. Introduction

Reasoning is an inherent part of human intelligence as it allows us to draw conclusions and construct explanations from existing knowledge when dealing with an uncertain scenario. One of the reasoning abilities that humans possess is abductive reasoning. Abductive reasoning aims to infer the most compelling explanation for a given set of observed facts. It is an extremely useful tool in our daily life, as we often rely on a set of facts to form the most probable conclusion. The ability to perform abductive reasoning about human actions is vital for human-robot collaborations. Imagine the scenario where a rescue robot enters an elderly person’s house to check on why he or she is not responding to the routine automated phone call. Upon entering the house, the robot observes its surroundings and notices that the *back door is left open* but *nothing else is out of the ordinary*. These observations may form a basis for a rational agent – the elderly might have *opened the door* and *went into the garden*. The robot can immediately make its way to search for him/her in the back garden. In this scenario, the rescue social robot may be able to verify if the

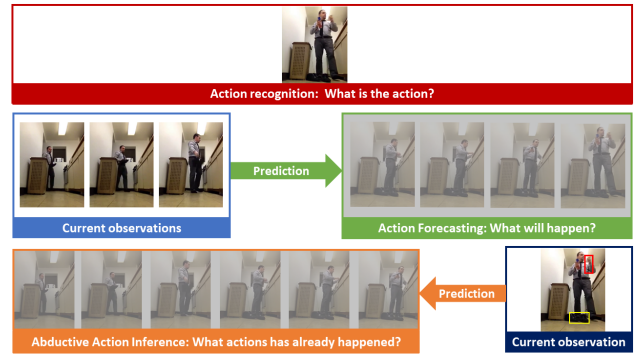


Figure 1: Different from works like action recognition (top) and action forecasting (middle), we ask the following question. Given a snapshot, what are the likely actions executed by the person before? As humans, we can infer that the person may have removed the shoes, and picked up a bottle. He may have opened the door and picked the box from the cabinet above. Even if the cabinet is partly visible, humans can derive these conclusions. This type of inference requires abductive reasoning; hence, we call this task abductive action inference (bottom).

person has been safe based on the factual observations in the scene and make conclusions based on logical abduction.

In recent years, there have been some great initiatives made in abductive reasoning for computer vision. In particular, [21] generates the description of the hypothesis and the premises in natural language given a video snapshot of events. Without the generation of a hypothesis description, these methods boil down to dense video captioning. A similar task is also presented in [15] where given an image, the model must perform logical abduction to explain the observation in natural language. However, these tasks involve natural language queries and may result in solving challenges related to language understanding, therefore, complicating the abductive reasoning task.

In contrast to these recent works, we challenge a model

to infer multiple human actions that may have occurred in the past from a given snapshot. Based on the visual information from the snapshot, objects such as a person, bottle, box, and shoes, may provide clues from which humans can draw conclusions. We term this new task, *Abductive Action Inference* and further benchmark how deep learning models perform on this challenging new task. For this task, the models are not only required to decipher the effects of human actions resulting in different environment states but also solve causal chains of action effects, a task that can be challenging even for humans. Furthermore, the task relies on the model’s ability to perform abductive reasoning based on factual evidence i.e., determining what actions may have or have not been performed based on visual information in the snapshot. Humans are able to solve this task by using prior experience (knowledge) about actions and their effects and use reasoning to make logical inferences. Are deep learning models able to perform abductive action inference by utilizing visual knowledge present in a given snapshot? We aim to answer this question in this paper.

Human action can be viewed as an evolution of human-object relationships over time. Therefore, the state of human-object relations in a scene may give away some cues about the actions that may have been executed by the human. We hypothesize that deep learning models are able to perform logical abduction on past actions using visual and semantic information of human-object relations in the scene. As these human-object relations provide substantial visual cues about actions, it makes it easier for the models to perform abductive reasoning. On the other hand, there is also the duality in which the evidence should support those conclusions (the actions inferred by the model). If a human executed a set of actions  $\mathcal{A}$  which resulted in a state whereby a human-object relation set  $\mathcal{R}$  is formed as an effect of those executed actions (i.e.,  $\mathcal{A} \rightarrow \mathcal{R}$ ), then using the relational information, we can formulate the task by aiming to infer  $\mathcal{A}$  from  $\mathcal{R}$ . Therefore, we argue that human-object relational representations are vital for abductive action inference and provide further justifications in our experiments.

In this work, our models rely on the human-centric object relation tuples such as (person, glass) and (person, closet) obtainable from a single image at the current point in time to perform abductive action inference. One can see why these human-centric relations are vital for identifying past actions: the (person, glass) relation may lead to deriving actions such as (person-pouring-water, person-took-glass-from-somewhere) while (person, closet) may imply actions such as (person-opening-closet, person-closing-closet) see – Figure 2. Therefore, we use objects and their relationships in the scene to construct human-centric object relations within each image. These relations are made up of both visual and semantic features (such as

Glove [24] embedding) of recognized objects. Our contributions are summarized as follows:

1. To the best of our knowledge, we are the first to propose the novel task of abductive action inference which is different from action recognition and forecasting – see Figure 1 and language-dependent visual abductive reasoning [21, 15].
2. We benchmark state-of-the-art (SOTA) image, video, vision-language, and object-relational models on this problem, thereby illustrating the importance of human-object relational representations for the task.
3. Lastly, we propose a novel Relational Bilinear graph encoder-decoder model to tackle this challenging reasoning problem.

## 2. Related Work

It should be noted that our work is different from action recognition [16, 14] in a fundamental way. First, in action recognition, the objective is to identify the actions executed in the visible data (e.g., a video or an image in still image action recognition [11]). In action recognition, the models can learn from visual cues what the action looks like and what constitutes an action. In our work, we aim to infer actions that the model has never seen the human performing. The model only sees visual evidence (e.g. human-object relations) in the scene which is the outcome of executed actions. There are no motion cues or visual patterns of actions that the model can rely on to abduct actions. From a single static image, the machine should infer what actions may have been executed. This is drastically different from classical action recognition and action anticipation tasks.

Abductive action inference has some similarity to short-term action anticipation [8, 6] and long-term action anticipation [1]. However, there are several notable differences between the two tasks. Firstly, in abductive action inference, the goal of the model is to identify the most plausible actions executed by a human based on the current evidence, whereas, in action anticipation, the model learns to predict future action sequences from current observations. Next, unlike action anticipation where a short video clip is typically observed (e.g. a 2-second-long video) before predicting future actions, in abductive action inference, we only process a single snapshot (frame) to perform abductive reasoning. In addition, predictive methods [12] are mostly used for action anticipation [10], whereas in abductive action inference, we are unable to use such predictive methods during training as we only have access to a single snapshot. Furthermore, while action anticipation has to deal with the uncertainty of human behavior in the future, in abductive action inference, the evidence (objects in the scene) may suggest what actions have been executed. Additionally, in abductive action inference, the uncertainty arises from the fact that several different actions may have resulted in sim-

ilar states  $\mathcal{R}$ . In our task, models should comprehend the consequences of each executed action and engage in reasoning to infer the most probable set or sequence of actions.

Visual Commonsense Reasoning (VCR) [36, 33] is also related to our work. In VCR [36], given an image, object regions, and a question, the model should answer the question regarding what is happening in the given frame. The model has to also provide justifications for the selected answer in relation to the question. Authors in [23] also studied a similar problem where a dynamic story underlying the input image is generated using commonsense reasoning. In particular, VisualCOMET [23] extends VCR and attempts to generate a set of textual descriptions of events at present, a set of commonsense inferences on events before, a set of commonsense inferences on events after, and a set of commonsense inferences on people’s intents at present. In this vein, given the complete visual commonsense graph representing an image, they propose two tasks; (1) generate the rest of the visual commonsense graph that is connected to the current event and (2) generate a complete set of commonsense inferences. In contrast, given a snapshot without any other natural language queries, we recognize visual objects in the scene and how they are related to the human and then use the human-centric relational representation to infer the most likely actions executed by the human.

Recently, there are machine learning models that can also perform logical reasoning. In particular, authors in [4] use abductive reasoning to improve the hypothesis of the learner. Furthermore, a neurosymbolic action recognition method that can generate some explanation for predicted actions is presented in [18]. Perhaps, our work is orthogonal to these ideas and our method can also benefit from these developed ideas. In VideoABC [37], models are required to infer the most plausible steps between two visual observations and provide reasons for less plausible steps. Differently, we ask the model to predict the set/sequence of actions from a single snapshot and verify if an action has been executed by a human to arrive at the current snapshot.

Visual scene graph generation [31] and spatial-temporal scene graph generation [3] are also related to our work. To be specific, any advancement made in scene graph generation, in particular, modeling relations between humans and objects should also help to improve the abductive action inference task as this task heavily relies on the human-object relations to perform abduction. Furthermore, situation understanding [34] is also related to our work. Graph neural networks are also related to our work [28, 35, 29]. However, our model relies on the Jaccard Vector Similarity to construct the affinity of the nodes and employs an encoder-decoder model. Our work is also related to bilinear pooling methods such as [9, 7]. However, we utilize bilinear pooling for relational modeling and abductive action inference.

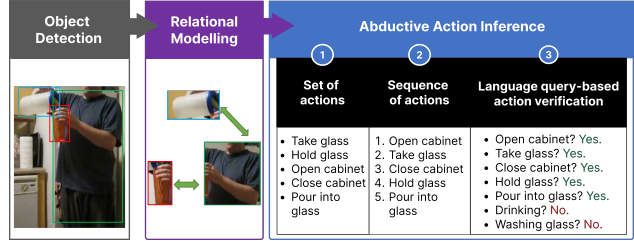


Figure 2: Proposed object-relational approach for abductive action inference. Models are tasked to: 1) abduct the set of actions, 2) abduct the sequence of actions, and 3) perform abductive action verification.

### 3. Abductive Action Inference

**Task:** Given a single snapshot, models have to infer the actions executed by the human up to the current moment in time using abductive reasoning which we coined Abductive Action Inference. Let us denote a human action by  $a_i \in A$  where  $A$  is the set of all actions and  $E_1, E_2, \dots$  is a collection of evidences from the evidence set  $\mathcal{E}$ . As the evidence is a result of actions, we can write the logical implication  $\mathcal{A} \rightarrow \mathcal{E}$  where  $\mathcal{A}$  is the set/sequence of actions executed by a human which resulted in a set of evidence  $\mathcal{E}$ . Then, the abductive inference task aims to derive 1) the set of actions, 2) the sequence of actions that resulted in the current evidence shown in the image (snapshot), and 3) abductive action verification. In abductive action verification, the model is given a single snapshot and is required to answer yes/no to an action query (did the person execute action  $a_x$ ?).

We benchmark three approaches to solve these tasks, 1) end-to-end trained models such as Slow-Fast networks [5], 2) vision-language models such as CLIP [25], BLIP [20], and 3) object-relational reasoning models. In the following subsections, we discuss the details of object-relational reasoning models and provide details on end-to-end training and vision-language models in the experiments section. We describe the details of abductive action set/sequence prediction, and verification using the object-relational approach.

#### 3.1. Object-Relational Representation Approach

Our primary hypothesis is that human-object relations are essential for abductive action inference. Therefore, we propose a human-object relational approach for the task. In all three tasks, our general approach is as follows. We first detect humans and objects in the snapshot and then generate a representation for human-centric object relations. Then, using these human-centric object relations, we summarize the visual snapshot, and using neural models, we infer the most likely actions executed by the human. The overview of this approach is shown in Figure 2. Here, we first discuss abductive action set inference, followed by the details of abductive action sequence inference and abductive action

verification.

**Abductive action set prediction:** Let us denote the object by  $o \in O$ , the predicate category by  $p \in P$ , and the human by  $h$ . The relation  $R$  is a triplet of the form  $\langle h, p, o \rangle$ . In each snapshot, we have  $n$  number of relations (these relations are the evidence  $\mathcal{E}$ ) and we seek to learn the following logical association:

$$a_1 \vee a_2 \vee a_3, \dots, \vee a_K \rightarrow R_1 \wedge R_2 \wedge \dots \wedge R_N \quad (1)$$

where  $R_1 \wedge R_2 \wedge \dots \wedge R_N$  is the relation set  $\mathcal{R}$  present in a situation and  $a_1 \vee a_2 \vee a_3, \dots, \vee a_K$  is the action set  $\mathcal{A}$  executed by the human to arrive at the situation. In this formulation, *the evidence is more structured* as it encompasses object relations. One might re-write this association as  $\mathcal{A} \rightarrow \mathcal{R}$  where  $\mathcal{R} \subset \mathbb{R}$  and  $\mathbb{R}$  is the set of all possible relations. Therefore, given  $\mathcal{R}$  we can perform abductive action inference to infer the most likely set of actions executed by the human.

We learn this logical association using the deep neural network functions  $\phi()$ , and  $\phi_c()$  of the following form by maximizing the conditional probability of

$$x_r = \phi(r_1, \dots, r_n; \theta_\phi) \quad (2)$$

$$P(a_1, \dots, a_K | r_1, \dots, r_n) = \phi_c(x_r; \theta_c) \quad (3)$$

where each  $r_k$  is a representation of the relation triplet  $R_k$  from a single snapshot,  $\phi$  is the relational model, and  $\phi_c$  is the linear classifier (or predictor). The training and inference sets comprise snapshots (images) and corresponding action set  $\mathcal{A}$ . From each snapshot, we extract the relation set  $\mathcal{R}_i$  and the action set  $\mathcal{A}_i$  that resulted in  $\mathcal{R}_i$ . Therefore, the dataset consists of  $\mathcal{D} = \bigcup_i \{\mathcal{R}_i, \mathcal{A}_i\}$ . Given the training set ( $\mathcal{D}$ ), we learn the model function in Equation 3 using backpropagation. For this task, we utilize the max-margin multi-label loss during training.

**Abductive action sequence prediction:** To generate the sequence of actions, we use the relational model  $\phi()$ , output  $x_r$ , and the classifier output  $\phi_c()$  and utilize a sequence decoder (GRU or Transformer) to generate the sequence of actions using element-wise cross-entropy loss during training. More details are given in section 4.6. Interestingly, this task requires the model to resolve causal chains of action effects when abducting the sequence of actions. Thus, this task is more challenging than action set prediction.

**Abductive action verification:** Abductive verification model  $\phi_{ver}()$  takes the evidence  $\mathcal{E}$  and the semantic representation of the action (e.g. textual encoding of the action name)  $y_a$  as inputs and outputs a binary classification score indicating if the evidence supports the action or not,

i.e.  $\phi_{ver}(\mathcal{E}, y_a) \rightarrow [0, 1]$ . Specifically, we encode the action name using the CLIP [25] text encoder to obtain the textual encoding  $y_a$  for action class  $a$ . Then, we concatenate  $y_a$  with  $x_r$  and utilize a two-layer MLP to perform binary classification to determine whether action  $a$  was executed or not. We use max-margin loss to train  $\phi_{ver}()$ .

### 3.2. Relational Representation

To obtain the relation representation, we extract features from the human and object regions of each snapshot (image) using a FasterRCNN [26] model with a ResNet101 backbone [13]. Let us denote the human feature by  $x_h$ , the object feature by  $x_o$ , and the features extracted from taking the union region of both human and object features by  $x_u$ . As we do not know the predicate or the relationship label for the relation between  $x_h$  and  $x_o$ , we use the concatenation of all three visual features  $x_h, x_o$ , and  $x_u$  as the joint relational visual feature  $x_v = [x_h, x_o, x_u]$ . Using FasterRCNN, we can also obtain the object and human categories. We use Glove [24] embedding to acquire a semantic representation of each human and object in the snapshot. Let us denote the Glove embedding of the human by  $y_h$  and the object by  $y_o$ . Then, the semantic representation of the relation is given by  $y_s = [y_h, y_o]$ . Using both visual and semantic representations, we obtain a joint representation for each human-centric relation in a given snapshot. Therefore, the default relation representation for a relation  $R = \langle h, p, o \rangle$  is given by  $r = [x_v, y_s]$ . Note that we do not have access to the predicate class or any information about the predicate. Next, we present several neural models for comparison.

### 3.3. Relational Transformer Model

Transformers [32] are a popular class of models in deep learning. They are very effective at capturing relationships between far apart elements in a set or a sequence. In this work, we use Transformers as a set summarization model. We use a multi-head self-attention Transformer model with one encoder and three decoder layers by default. We do not use any positional encoding as we are summarising a set. Given the set of relational representation of an image  $\mathcal{R}_i = r_1, r_2, \dots, r_n$ , the Transformer model outputs a Tensor of size  $n \times d$  where  $d$  is the size of the relational representation. Afterward, we use max-pooling to obtain a snapshot representation vector  $x_r$ .

### 3.4. GNED: Relational Graph Neural Network

In our work, the graph neural network based encoder-decoder model summarizes relational information for abductive action inference. Given the relational data with slight notation abuse, let us denote the relational representations by a  $n \times d$  matrix  $\mathcal{R} = [r_1, r_2, \dots, r_n]$  where  $r_n$  has  $d$  dimensions. In our graph neural network encoder-decoder (GNED) model, we first project the relational data using

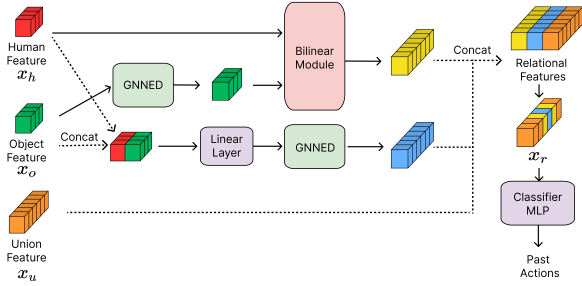


Figure 3: The BiGED architecture.

a linear function as follows:

$$\mathcal{R}' = \mathcal{R}W_l + b_l \quad (4)$$

where  $\mathcal{R}' = [r'_1, r'_2, \dots, r'_n]$ . Then, we construct the affinity matrix  $W_A(i, j)$  using Jaccard Vector similarity, where  $W_A(i, j)$  shows the similarity/affinity between the  $i$ -th relation and the  $j$ -th relation in the set. Here, we use Jaccard Vector Similarity which is a smooth and fully differentiable affinity [6]. Note that Jaccard Vector Similarity is bounded by  $[-1, 1]$ . Here,  $a \cdot b$  denotes the dot product. Thereafter, we obtain the graph-encoded relational representation as follows:

$$G_e = \text{ReLU}((W_A \mathcal{R}')W_g + b_g) \quad (5)$$

where  $W_g$  and  $b_g$  are the weight matrix and bias term respectively. We call equations 4-5 the graph module. Using the graph module as a base model, we develop a graph encoding layer. We refer the user to the supplementary materials for details on the GNNED architecture. Our graph encoder-decoder model consists of one graph encoder, and three graph decoders by default. The graph module is able to model the inter-relations between human-object relations and reasons about them to perform abduction on actions. Finally, we apply max-pooling at the end of the graph encoder-decoder model to obtain the final snapshot representation  $x_r$ .

### 3.5. RBP: Relational bilinear pooling

To effectively model the higher-order relational information between human and object features, we use bilinear pooling. Given the human representation  $x_h$  and the object representation  $x_o$ , we use bilinear pooling with a weight matrix  $W_b$  of size  $d \times d \times d$  and linear projection matrices  $W_{bl}, W_{jb}$  as follows:

$$o' = \text{ReLU}(W_o x_o + b_o) \quad (6)$$

$$h' = \text{ReLU}(W_h x_h + b_h) \quad (7)$$

$$r_b = \text{ReLU}([h'W_b o'; ([h'; o']W_{bl} + b_{bl})])W_{jb} + b_{jb} \quad (8)$$

where  $[\cdot]$  represents the vector concatenation and  $h'W_b o'$  is the bilinear pooling operator applied over human and

object features.  $([o'; h']W_{bl} + b_{bl})$  is the output of concatenated human and object features followed by a linear projection using weight matrix  $W_{bl}$  and bias term  $b_{bl}$ . In contrast to bilinear pooling, the concatenated linear projection captures direct relational information between human and object features. Then, we concatenate the bilinear pooled vector  $(h'W_b o')$  and the output of the linear projection  $([o'; h']W_{bl} + b_{bl})$ . Then, we use ReLU and apply another linear projection  $(W_{jb} + b_{jb})$ . Finally, we concatenate the overlap feature  $x_u$  with the overall model output  $(r_b)$  and apply max-pooling across all relational features  $([r_b; x_u])$  in the image to obtain  $x_r$ .

### 3.6. BiGED: Bilinear Graph Encoder-Decoder

Finally, to take advantage of both bilinear relational modeling and graph neural network encoder-decoder models, we combine both strategies. The main idea is to replace the projection function in Equation 6 with a graph neural network encoder-decoder model. Let us denote the graph neural network encoder-decoder model by  $f_{Ged}(\cdot)$ . Then, equation 6 will be replaced as follows:

$$O' = f_{Ged}(X_o) \quad (9)$$

where  $X_o$  is all the object features in the snapshot. Afterward, we apply equation 8 before using bilinear modeling to obtain the relational representation. Note that as there are only one or two humans in the snapshot, we do not use the GNNED to model human features. We concatenate the original human and object features  $[x_h, x_o]$  to obtain a joint feature and then pass it through a linear layer and another GNNED model. The outputs of the bilinear, joint feature-based GNNED models and overlap union feature  $x_u$  are concatenated to obtain the final relational representation. A visual illustration of this model is shown in Figure 3. Afterward, we use max-pooling to obtain the representation  $x_r$  for the snapshot. For all models, we employ a linear classifier to infer past actions using the representation vector  $x_r$ .

## 4. Experiments and Results

### 4.1. Dataset

We benchmark all models on the Action Genome (AG) dataset [17] for abductive action inference tasks. Built upon the Charades dataset [30], the AG dataset contains 9,848 videos with 476,000+ object bounding boxes and 1.72 million visual relationships annotated across 234,000+ frames. The original objective of this dataset is to study spatial-temporal scene graph generation. *It should be noted that not all video frames in the Charades dataset are used in the AG dataset. Only a handful of key frames are used in AG, and we follow the same.* The AG dataset does not provide action annotations. To obtain action annotations for snapshots of AG, we leverage the Charades dataset which con-

Model	mAP	R@10	mR@10
Human Performance	–	80.60	82.81
<b>End-to-end training</b>			
Slow-Fast [5]	7.91	14.42	7.65
ResNet101-2D [13]	9.27	18.63	11.51
Resnet50-3D [5]	8.16	16.08	7.83
<b>Vision-language models</b>			
CLIP-ViT-B/32 (zero shot) [25]	14.07	14.88	20.88
CLIP-ViT-L/14 (zero shot) [25]	19.79	21.88	27.77
CLIP-ViT-B/32 (linear probe) [25]	16.16	31.25	16.38
CLIP-ViT-L/14 (linear probe) [25]	22.06	40.18	20.01
BLIP (vqa) [20]	6.18	9.84	15.76
<b>Object-relational methods - using gt human/objects</b>			
Relational Rule-based inference	26.27	48.94	36.89
Relational MLP	27.73	42.50	25.80
Relational Transformer	33.59	56.03	40.04
Relational GNNED	34.38	57.17	42.83
RBP	35.55	59.98	43.53
Action Anticipation [6]	34.41	53.40	41.84
BiGED	<b>35.75</b>	<b>60.55</b>	<b>44.37</b>
<b>Object-relational method - using FasterRCNN labels</b>			
BiGED	<b>24.13</b>	<b>43.59</b>	<b>30.12</b>

Table 1: Abductive action set inference performance using the proposed methods on the *Abduct at T* setup.

tains 157 action classes. To be specific, we use frame-level action annotations from Charades to get the action annotations for AG snapshots. Then, we construct the training and testing dataset for abductive action inference. We provide details on how to generate the action set and sequences in the supplementary materials.

## 4.2. Experimental Setup

After obtaining the action annotations of snapshots for a given video, we drop videos having only one snapshot as there are no past snapshots and therefore, no past actions. For the remaining snapshots, we assign action labels from the previous snapshots in two different evaluation setups:

**1. Abduct at  $T$ :** Given a snapshot at time  $T$ , we add action labels from all the previous snapshots (frames) to the ground truth (including actions from the current snapshot) where  $\mathcal{A}_t$  denotes all actions of the  $t^{th}$  snapshot. Therefore,

the ground truth action set  $\mathcal{A}$  is given by  $\mathcal{A} = \bigcup_{t=1}^T \mathcal{A}_t$ .

**2. Abduct last snapshot:** Based on the first setup, we add an additional task where the model has to perform inference only on the last snapshot of each video which contains all past actions. If the last snapshot is  $T'$ , then the action set is

$\mathcal{A} = \bigcup_{t=1}^{T'} \mathcal{A}_t$ . Note that in the Action Genome dataset, the snapshots are sampled non-homogeneously from the Charades dataset videos. Therefore, the previous snapshot occurs several seconds before the current snapshot. In our abductive action inference task, the ground truth action sets are confined to the length of each video. We provide details on the number of snapshots for a set of  $n$  past actions in the AG dataset for these setups in the supplementary materials.

First, we utilize the mean Average Precision (mAP), Re-

Model	mAP	R@10	mR@10
Relational Rule-based inference	26.18	44.34	33.94
Relational MLP	25.99	38.79	23.54
Relational Transformer	30.13	47.55	35.05
Relational GNNED	30.95	48.18	36.36
RBP	31.48	<b>49.79</b>	<b>36.96</b>
BiGED	<b>31.55</b>	49.62	36.15

Table 2: Abductive action set inference performance using the proposed methods on the *Abduct last snapshot* setup.

call@K (R@K), and mean Recall@K (mR@K) metrics<sup>1</sup> to evaluate the models for the abductive action set prediction and action verification tasks. K is set to 10 based on the average number of actions contained in a snapshot. Each snapshot contains 8.9 and 8.2 actions for *Abduct at T* and *Abduct last snapshot* setups for the abductive inference set and action verification tasks. Lastly, we use the accuracy metric to evaluate the action sequence prediction models.

## 4.3. Implementation Details

We use FasterRCNN [26] with a ResNet101 [13] backbone to extract human and object features from each snapshot based on the ground truth person and object bounding boxes provided by AG for all object-relational models. We load pre-trained weights provided by [3] that were trained on the training set of AG which obtained 24.6 mAP at 0.5 IoU with COCO metrics. The parameters of the FasterRCNN during training and inference are fixed for the abductive action inference task. Our default human and object visual representations have 512 dimensions obtained from 2048 dimensional visual features from the FasterRCNN. We use linear mappings to do this. During training, we train the models for 10 epochs and set the batch size to 1 video (there are many frames in a video). We assume the frames are i.i.d. Note that even though there are multiple snapshots in a batch, the snapshots are processed in parallel and individually for the transformer and graph models respectively. There is no sharing of information between snapshots. We use the AdamW [22] optimizer with an initial learning rate of 1e-5 along with a scheduler to decrease the learning rate by a factor of 0.5 to a minimum of 1e-7. We utilize Glove [24] word embedding of size 200 for object and subject (human) semantic features. In addition, gradient clipping with a maximal norm of 5 is applied. Moreover, we report the mean across 3 different runs for each configuration to ensure we report the most accurate performance of our models. All models (except end-to-end) are trained on a single RTX3090 or A5000 GPU. For CLIP, we use publicly available implementations [25].

<sup>1</sup>see supplementary material for details.

#### 4.4. Baseline Models

We benchmark three publicly available image (Resnet101-2D) and video models (Slow-Fast and Resnet50-3D) using their official implementations. Image models are pre-trained on ImageNet [27] while video models are pre-trained on Kinetics400 [19] dataset and we fine-tune these models on our task. We use batch size of 32 with a learning rate of  $1e-5$ . For video-based methods, we select the surrounding 8 frames of a snapshot from the Charades dataset to fine-tune these models end-to-end. We also use CLIP linear-probe and zero-shot to perform abduction using several variants of the CLIP model [25]. We also evaluate the BLIP [20] model using question answering (inference with generate option) on this task. We also benchmark against three additional object-relational baseline models, 1) Multi-Layered Perceptron (MLP) and 2) rule-based 3) an action anticipation model that correlates past observations with the present [6]. Details of these models and the human performance evaluation process are provided in the supplementary materials.

#### 4.5. Evaluation of Abductive Action Set Prediction

Our results for the abductive action inference set prediction task is shown in Table 1. These results are obtained based on the *Abduct at T* setup. During training, the model learns from every single snapshot in the video sequence independently. Likewise, during inference, the model predicts the past action set on every single snapshot. The end-to-end trained models such as Slow-Fast [5], ResNet50-3D, and Resnet101-2D perform poorly as it may be harder for these models to find clues that are needed for the abductive inference task. On the other hand, multi-modal foundational models such as the CLIP [25] variants are able to obtain better results than vanilla CNN models on this task. Interestingly, even the simplest object-relational models such as MLP and rule-based inference methods outperform the CLIP model. One might argue that the performance of human-object relational models is attributed to the use of ground truth object labels in the scene. However, when we tried to incorporate ground truth objects in the CLIP [25] model, performance was poor. Therefore, we conclude that the CLIP and BLIP models are not suited for abductive inference tasks even though CLIP is able to perform well due to its excellent generalization ability.

The results also suggest that the human-object relational representations provide valuable evidence (cues) about what actions may have been executed in contrast to holistic vision representations. Among object-relational models, the MLP model and rule-based inference perform the worst across all three metrics. The Relational Transformer model improves results over MLP. Furthermore, the Relational GNNED improves the results by 0.79, 1.14, and 2.8 respectively over Transformer. Surprisingly, the RBP ob-

Model	Accuracy	
Human performance	14.00	
	GRU	Transformer
Relational MLP	9.43	9.59
Relational Transformer	9.71	9.95
Relational GNNED	9.81	10.11
RBP	10.48	10.22
BiGED	10.54	10.15

Table 3: Abductive action sequence prediction using the proposed methods on the *Abduct at T* setup.

tains particularly good results outperforming the previous models across all three metrics. The GNNED and RBP models follow two different approaches which capture relational information and the way the relational reasoning is performed is fundamentally different. Yet, these models obtain better results than the Transformer model. Finally, the combination of both GNNED and RBP, i.e., BiGED performs even better. An action anticipation model that correlates past observations with the future [6] also performs well using relational features. However, this model has access to prior snapshots during training which other models did not use. All object-relational models use the ground truth object labels from the AG dataset to obtain semantic representations. We observe a drop in performance when we use predicted objects from the FasterRCNN model. Nevertheless, the performance of BiGED with FasterRCNN labels is significantly better than end-to-end trained models and vision-language models. Finally, it should be emphasized that the human performance on this task is significantly better than any of the modern AI models.

Next, we evaluated the model’s performance on the second setup where the model has to *perform abduction on the last snapshot of each video*. However, we only focus on object-relational methods. To be specific, we use the trained models in the previous setup directly for inference. As a myriad of actions could have happened throughout a video sequence, this setup is particularly challenging. The results of this task are shown in Table 2. We observe that the results are lower than the previous setup for all models, which demonstrates that the task is indeed more challenging. The MLP model and the rule-based inference have relatively poor performance. Still, the GNNED, RBP, and BiGED methods have better performance than the Transformer model despite the GNNED having a similar architecture to the Transformer. Although the BiGED obtains the best performance for mAP, we note that the best performing model for R@10 and mR@10 is the RBP model.

#### 4.6. Evaluation of Action Sequence Prediction

Next, we formulated the abductive action sequence prediction task based on the *Abduct at T* setup. We attached a 2-layer GRU / Transformer decoder to our existing object-



Snapshot	MLP	Transformer	GNNED	RBP	BiGED
	Holding a dish Taking a cup/glass/bottle from somewhere Holding a cup/glass/bottle of something Working/Playing on a laptop Working at a table Watching a laptop or something on a laptop Drinking from a cup/glass/bottle	Holding a dish Taking a cup/glass/bottle from somewhere Holding a cup/glass/bottle of something Working/Playing on a laptop Working at a table Watching a laptop or something on a laptop Drinking from a cup/glass/bottle	Holding a dish Taking a cup/glass/bottle from somewhere Holding a cup/glass/bottle of something Working/Playing on a laptop Working at a table Watching a laptop or something on a laptop Drinking from a cup/glass/bottle	Holding a dish Taking a cup/glass/bottle from somewhere Holding a cup/glass/bottle of something Working/Playing on a laptop Working at a table Watching a laptop or something on a laptop Drinking from a cup/glass/bottle	Holding a dish Taking a cup/glass/bottle from somewhere Holding a cup/glass/bottle of something Working/Playing on a laptop Working at a table Watching a laptop or something on a laptop Drinking from a cup/glass/bottle
	Holding a blanket Holding a bag Snuggling with a blanket Sitting on the floor Lying on the floor Holding a vacuum Someone is awakening somewhere	Holding a blanket Holding a bag Snuggling with a blanket Sitting on the floor Lying on the floor Holding a vacuum Someone is awakening somewhere	Holding a blanket Holding a bag Snuggling with a blanket Sitting on the floor Lying on the floor Holding a vacuum Someone is awakening somewhere	Holding a blanket Holding a bag Snuggling with a blanket Sitting on the floor Lying on the floor Holding a vacuum Someone is awakening somewhere	Holding a blanket Holding a bag Snuggling with a blanket Sitting on the floor Lying on the floor Holding a vacuum Someone is awakening somewhere

Figure 4: Qualitative results produced by each model on the Abductive action set inference *Abduct last snapshot* setup on the AG test dataset. The first column shows the snapshot. The remaining columns show the actions predicted by each model. Actions highlighted in green are correctly inferred while the rest are ground truth actions that the model did not infer.

Model	mAP	R@10	mR@10
Human Performance	–	92.26	93.71
Relational MLP	26.58	41.71	25.40
Relational Transformer	27.94	45.72	30.12
RBP	32.19	53.76	38.44
BiGED	34.13	57.39	41.97

Table 4: Abductive action verification performance using the proposed methods on the *Abduct at T* setup.

relational models (in Table 2). To train both sequence prediction models, we freeze the object detector and relational model ( $\phi()$ ). Then, we use the relational vector  $x_r$  and action distribution obtained from  $\phi_c()$  in Eq. 3 as the initial hidden state and input to the GRU respectively. The transformer decoder takes non-pooled relational features (a matrix of size  $n \times d$ ) as the key, value, and max-pooled relational features  $x_r$  as the query. The output of these models are fed into a linear classifier to produce action sequences autoregressively. The results of these models are reported in Table 9. The BiGED model obtains slightly better performance than the rest. Although the performances of these models are suboptimal, we note that humans are also unable to obtain satisfactory results (only 14.00% accuracy). As we are constrained to only utilize available information in a single frame, the solution contains a substantial amount of sequence permutations. Therefore, making the task extremely challenging.

#### 4.7. Evaluation of Abductive Action Verification

We present abductive action verification results in Table 4 using the object-relational approach. As before, we use the ground truth human and object class names to ob-

tain the semantic representation. As the query is in textual form (i.e. the action class name), we suggest that the abductive action verification resembles a human-like task. It is easy to answer yes, or no to the question "Did the person execute action  $a_i$  in this snapshot to arrive at this state?" Interestingly, the performance of this task is slightly lower than the main results we obtained in Table 1. Even though this task is mentally easier for the human, it seems the task is slightly difficult for the machine as it now has to understand the complexities of human languages.

#### 4.8. Qualitative Results

We compare qualitative results for the abductive action set prediction task in Figure 4. Depending on the number of past action labels a snapshot has, we take the same number of top-k predicted actions from each model. All models demonstrate their ability to perform abductive action inference. In the first snapshot, there are objects such as a person, laptop, table, cup, and dish. In the second snapshot, there are objects such as a person, floor, blanket, bag, and vacuum. In both scenarios, RBP and BiGED demonstrate that they can infer actions more accurately.

### 5. Discussion & Conclusion

This paper introduced a new task called abductive action inference which comprises three sub-problems namely: action set/sequence prediction and action verification. Our experiments demonstrate that deep learning models are able to perform abductive action inference to a certain extent. Moreover, we showed that end-to-end trained holistic representational models are not effective in this task. In addi-



tion, although large-scale multi-modal foundational models such as CLIP [25] show some promising results, our proposed human-object relational modeling methods such as relational graph neural networks, relational bilinear pooling and their combination, BiGED outperform these existing models. This reveals the effectiveness of object-relational models for abductive action inference. This is a challenging AI research problem and therefore, we believe this research question deserves deeper investigation.

## References

- [1] Yazan Abu Farha, Alexander Richard, and Juergen Gall. When will you do what?-anticipating temporal occurrences of activities. In *Proceedings of the IEEE conference on computer vision and pattern recognition*, pages 5343–5352, 2018.
- [2] Jimmy Lei Ba, Jamie Ryan Kiros, and Geoffrey E Hinton. Layer normalization. *arXiv preprint arXiv:1607.06450*, 2016.
- [3] Yuren Cong, Wentong Liao, Hanno Ackermann, Bodo Rosenhahn, and Michael Ying Yang. Spatial-temporal transformer for dynamic scene graph generation. In *Proceedings of the IEEE/CVF International Conference on Computer Vision*, pages 16372–16382, 2021.
- [4] Wang-Zhou Dai, Qiuling Xu, Yang Yu, and Zhi-Hua Zhou. Bridging machine learning and logical reasoning by abductive learning. *Advances in Neural Information Processing Systems*, 32, 2019.
- [5] Christoph Feichtenhofer, Haoqi Fan, Jitendra Malik, and Kaiming He. Slowfast networks for video recognition. In *Proceedings of the IEEE/CVF international conference on computer vision*, pages 6202–6211, 2019.
- [6] Basura Fernando and Samitha Herath. Anticipating human actions by correlating past with the future with jaccard similarity measures. In *Proceedings of the IEEE/CVF Conference on Computer Vision and Pattern Recognition*, pages 13224–13233, 2021.
- [7] Akira Fukui, Dong Huk Park, Daylen Yang, Anna Rohrbach, Trevor Darrell, and Marcus Rohrbach. Multimodal compact bilinear pooling for visual question answering and visual grounding. *arXiv preprint arXiv:1606.01847*, 2016.
- [8] Antonino Furnari and Giovanni Maria Farinella. What would you expect? anticipating egocentric actions with rolling-unrolling lstms and modality attention. In *Proceedings of the IEEE/CVF International Conference on Computer Vision*, pages 6252–6261, 2019.
- [9] Yang Gao, Oscar Beijbom, Ning Zhang, and Trevor Darrell. Compact bilinear pooling. In *Proceedings of the IEEE Conference on Computer Vision and Pattern Recognition (CVPR)*, June 2016.
- [10] Rohit Girdhar and Kristen Grauman. Anticipative video transformer. In *Proceedings of the IEEE/CVF International Conference on Computer Vision*, pages 13505–13515, 2021.
- [11] Guodong Guo and Alice Lai. A survey on still image based human action recognition. *Pattern Recognition*, 47(10):3343–3361, 2014.
- [12] Tengda Han, Weidi Xie, and Andrew Zisserman. Video representation learning by dense predictive coding. In *Proceedings of the IEEE/CVF International Conference on Computer Vision Workshops*, pages 0–0, 2019.
- [13] Kaiming He, Xiangyu Zhang, Shaoqing Ren, and Jian Sun. Deep residual learning for image recognition. In *Proceedings of the IEEE conference on computer vision and pattern recognition*, pages 770–778, 2016.
- [14] Samitha Herath, Mehrtash Harandi, and Fatih Porikli. Going deeper into action recognition: A survey. *Image and vision computing*, 60:4–21, 2017.
- [15] Jack Hessel, Jena D Hwang, Jae Sung Park, Rowan Zellers, Chandra Bhagavatula, Anna Rohrbach, Kate Saenko, and Yejin Choi. The abduction of sherlock holmes: A dataset for visual abductive reasoning. *arXiv preprint arXiv:2202.04800*, 2022.
- [16] Hueihan Jhuang, Juergen Gall, Silvia Zuffi, Cordelia Schmid, and Michael J Black. Towards understanding action recognition. In *Proceedings of the IEEE international conference on computer vision*, pages 3192–3199, 2013.
- [17] Jingwei Ji, Ranjay Krishna, Li Fei-Fei, and Juan Carlos Niebles. Action genome: Actions as compositions of spatio-temporal scene graphs. In *Proceedings of the IEEE/CVF Conference on Computer Vision and Pattern Recognition*, pages 10236–10247, 2020.
- [18] Yang Jin, Linchao Zhu, and Yadong Mu. Complex video action reasoning via learnable markov logic network. In *Proceedings of the IEEE/CVF Conference on Computer Vision and Pattern Recognition*, pages 3242–3251, 2022.
- [19] Will Kay, Joao Carreira, Karen Simonyan, Brian Zhang, Chloe Hillier, Sudheendra Vijayanarasimhan, Fabio Viola, Tim Green, Trevor Back, Paul Natsev, et al. The kinetics human action video dataset. *arXiv preprint arXiv:1705.06950*, 2017.
- [20] Junnan Li, Dongxu Li, Caiming Xiong, and Steven Hoi. Blip: Bootstrapping language-image pre-training for unified vision-language understanding and generation. In *International Conference on Machine Learning*, pages 12888–12900. PMLR, 2022.
- [21] Chen Liang, Wenguan Wang, Tianfei Zhou, and Yi Yang. Visual abductive reasoning. In *Proceedings of the IEEE/CVF Conference on Computer Vision and Pattern Recognition*, pages 15565–15575, 2022.
- [22] Ilya Loshchilov and Frank Hutter. Decoupled weight decay regularization. *arXiv preprint arXiv:1711.05101*, 2017.
- [23] Jae Sung Park, Chandra Bhagavatula, Roozbeh Mottaghi, Ali Farhadi, and Yejin Choi. Visualcomet: Reasoning about the dynamic context of a still image. In *European Conference on Computer Vision*, pages 508–524. Springer, 2020.
- [24] Jeffrey Pennington, Richard Socher, and Christopher D Manning. Glove: Global vectors for word representation. In *Proceedings of the 2014 conference on empirical methods in natural language processing (EMNLP)*, pages 1532–1543, 2014.
- [25] Alec Radford, Jong Wook Kim, Chris Hallacy, Aditya Ramesh, Gabriel Goh, Sandhini Agarwal, Girish Sastry, Amanda Askell, Pamela Mishkin, Jack Clark, et al. Learning

- transferable visual models from natural language supervision. In *International conference on machine learning*, pages 8748–8763. PMLR, 2021.
- [26] Shaoqing Ren, Kaiming He, Ross Girshick, and Jian Sun. Faster r-cnn: Towards real-time object detection with region proposal networks. *Advances in neural information processing systems*, 28, 2015.
- [27] Olga Russakovsky, Jia Deng, Hao Su, Jonathan Krause, Sanjeev Satheesh, Sean Ma, Zhiheng Huang, Andrej Karpathy, Aditya Khosla, Michael S. Bernstein, Alexander C. Berg, and Li Fei-Fei. Imagenet large scale visual recognition challenge. *CoRR*, abs/1409.0575, 2014.
- [28] Franco Scarselli, Marco Gori, Ah Chung Tsoi, Markus Hagenbuchner, and Gabriele Monfardini. The graph neural network model. *IEEE transactions on neural networks*, 20(1):61–80, 2008.
- [29] Michael Schlichtkrull, Thomas N Kipf, Peter Bloem, Rianne van den Berg, Ivan Titov, and Max Welling. Modeling relational data with graph convolutional networks. In *European semantic web conference*, pages 593–607. Springer, 2018.
- [30] Gunnar A Sigurdsson, Gül Varol, Xiaolong Wang, Ali Farhadi, Ivan Laptev, and Abhinav Gupta. Hollywood in homes: Crowdsourcing data collection for activity understanding. In *European Conference on Computer Vision*, pages 510–526. Springer, 2016.
- [31] Kaihua Tang, Yulei Niu, Jianqiang Huang, Jiaxin Shi, and Hanwang Zhang. Unbiased scene graph generation from biased training. In *Proceedings of the IEEE/CVF conference on computer vision and pattern recognition*, pages 3716–3725, 2020.
- [32] Ashish Vaswani, Noam Shazeer, Niki Parmar, Jakob Uszkoreit, Llion Jones, Aidan N Gomez, Łukasz Kaiser, and Illia Polosukhin. Attention is all you need. *Advances in neural information processing systems*, 30, 2017.
- [33] Aming Wu, Linchao Zhu, Yahong Han, and Yi Yang. Connective cognition network for directional visual commonsense reasoning. *Advances in Neural Information Processing Systems*, 32, 2019.
- [34] Mark Yatskar, Luke Zettlemoyer, and Ali Farhadi. Situation recognition: Visual semantic role labeling for image understanding. In *Proceedings of the IEEE conference on computer vision and pattern recognition*, pages 5534–5542, 2016.
- [35] Changqian Yu, Yifan Liu, Changxin Gao, Chunhua Shen, and Nong Sang. Representative graph neural network. In *European Conference on Computer Vision*, pages 379–396. Springer, 2020.
- [36] Rowan Zellers, Yonatan Bisk, Ali Farhadi, and Yejin Choi. From recognition to cognition: Visual commonsense reasoning. In *Proceedings of the IEEE/CVF conference on computer vision and pattern recognition*, pages 6720–6731, 2019.
- [37] Wenliang Zhao, Yongming Rao, Yansong Tang, Jie Zhou, and Jiwen Lu. Videoabc: A real-world video dataset for abductive visual reasoning. *IEEE Transactions on Image Processing*, 31:6048–6061, 2022.

## 6. Supplementary Material

Here, we describe the process of generating action sets and sequences using the images from the Action Genome and action labels from the Charades dataset for the abductive inference task. Additionally, we present the frequency distribution on the number of past actions for each snapshot on the *Abduct at T*, and *Abduct last snapshot* setups for action set prediction. We also include the number of past actions for each snapshot on the *Abduct at T* setup for abductive action sequence prediction. Note that the action verification task utilizes the same ground truth labels as the set prediction task. Then, we discuss how we go about performing the human experiments for the *Abduct at T* setup for action prediction, sequence prediction, and action verification. Afterward, we provide details of the object-relational methods such as MLP and rule-based inference for abductive action inference. We also include the graph neural network encoder-decoder architecture and further expand on its similarities to the Transformer model. Next, we describe and include the GRU and Transformer decoder used for the action sequence inference task. Subsequently, we discuss the evaluation metric calculation for the abductive inference tasks. Then, we report additional quantitative and conduct several ablation studies for our object-relational models. Lastly, we also show additional qualitative results for the abductive set inference task.

### 6.1. How to generate action sets and sequences?

In both tasks, to obtain the ground truth action set  $\mathcal{A}$  for a snapshot in the Action Genome dataset using the Charades action labels, we first compute the time  $t$  for each individual frame within a video sequence by using the formula:

$$t = \frac{v_d}{n} \quad (10)$$

where  $v_d$  and  $n$  denote the video duration and the number of frames in the video respectively. Then, we multiply the current frame number  $f_n$  with  $t$  to obtain the current time:

$$t_c = t \times f_n \quad (11)$$

**Action sets:** As each video contains multiple actions, we check whether the current time of the frame  $t_c$ , falls within the start  $t_s$  and end  $t_e$  time of the action. If it does, we add the ground truth action label to the action set  $\mathcal{A}_n$  for the snapshot. To obtain the ground truth action set for the  $t^{\text{th}}$  snapshot, we combine all previous action sets from  $t = 1$  up to and including the  $t^{\text{th}}$  snapshot to form the set.

**Action sequences:** We sort the start time  $t_s$  of the actions contained in the video in ascending order. Then, for each snapshot, if the current time of the frame is greater than the start time of the action ( $t_c \geq t_s$ ), we add it to the sequence.

### 6.2. Set of past actions

As mentioned in the experimental setup section of our paper, we present the set of  $n$  past actions for the *Abduct at T* and *Abduct last snapshot*. In addition, we also provide an additional setup *Abduct previous and current snapshot* in Figure 5. Note that a snapshot contains up to 26 actions for *Abduct at T* and *Abduct last snapshot* setups while *Abduct from previous and current snapshot* contains up to 19 actions. Note that the action verification task uses the same set of ground truth action labels from the set of past actions.

### 6.3. Sequence of past actions

We also provide the number of actions  $n$  for each snapshot for the abductive action sequence inference task. Each snapshot contains up to 28 actions. The average number of actions in a snapshot is 6.5. For more information, refer to Figure 6.

### 6.4. Human Performance Evaluation

We report the human performance on the abductive action inference set, sequence, and verification tasks for the *Abduct at T* setup in our main paper in Tables 1, 3, and 4. All human experiments for the three sub-problems based on the *Abduct at T* setup are executed in the same manner. First, we randomly sample 100 test snapshots and manually go through every action class in the Charades dataset without looking at the ground truth for each snapshot. Then, we select the set of actions that are likely to have occurred before the snapshot. Then, following our main paper, we compute the evaluation metrics outlined in the supplementary material section 6.10.

### 6.5. Rule-based Inference

In abductive action inference, we aim to learn the following logical association

$$a_1 \vee a_2 \vee a_3, \dots, \vee a_K \rightarrow R_1 \wedge R_2 \wedge \dots \wedge R_N \quad (12)$$

where  $R_1 \wedge R_2 \wedge \dots \wedge R_N$  is the relation set  $\mathcal{R}$  present in a snapshot and  $a_1 \vee a_2 \vee a_3, \dots, \vee a_K$  is the action set  $\mathcal{A}$  executed by the human to arrive at the snapshot. Note the set of all actions is denoted by  $A$  where  $\mathcal{A} \subset A$ .

In Rule-based Inference, each relation is in the symbolic form  $R_k = \langle H, o_k \rangle$  where  $H$  and  $o_k$  are the human feature and  $k^{\text{th}}$  **object label** in the snapshot. As the human feature is common in all relations, we omit the human feature in each relation. Then, the relational association is updated as follows:

$$a_1 \vee a_2 \vee a_3, \dots, \vee a_K \rightarrow o_1 \wedge o_2 \wedge \dots \wedge o_N \quad (13)$$

for any snapshot. In rule-based abductive action set inference, for each given object pattern (also the relation pattern)

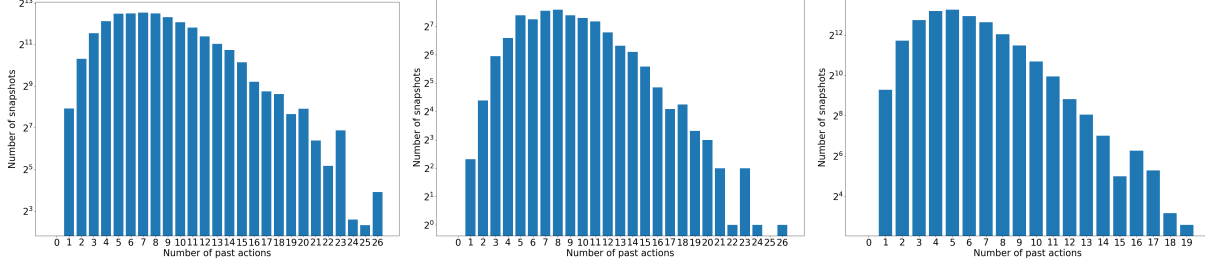


Figure 5: Number of snapshots (in  $\log_2$ ) for sets of  $n$  past actions in the Action Genome test set. (a) – *Abduct at T*, (b) – *Abduct last snapshot* and (c) – *Abduct current and previous snapshots* setups.

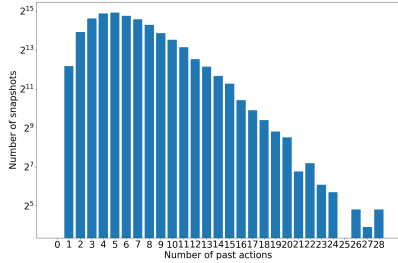


Figure 6: Number of snapshots (in  $\log_2$ ) for sets of  $n$  past actions in the Action Genome test set for the abductive action sequence prediction task with *Abduct at T* setup.

$o_1 \wedge o_2 \wedge \dots \wedge o_N$ , we count the occurrence of each action  $a_j$ . Let us denote the frequency of action  $a_j$  for object pattern  $\mathcal{O}_q = o_1 \wedge o_2 \wedge \dots \wedge o_N$  from the entire training set by  $C_j^q$ . Therefore, for each object pattern  $\mathcal{O}_q$ , we obtain a frequency vector over all actions denoted by:

$$\mathbf{C}^q = [C_1^q, C_2^q, \dots, C_{|A|}^q] \quad (14)$$

Then, we can convert these frequencies into probabilities using softmax:

$$P(A|\mathcal{O}_q) = \text{softmax}([C_1^q, C_2^q, \dots, C_{|A|}^q]) \quad (15)$$

We use this to perform abductive action set inference using the test set. Given a test snapshot, we first obtain the object pattern  $\mathcal{O} = o_1 \wedge o_2 \wedge \dots \wedge o_N$ . Next, we obtain the action probability vector for the object pattern from the training set using Equation 15. If an object pattern does not exist in the training set, we assign equal probability to each action.

## 6.6. Relational MLP

The MLP proposed consists of 2-layers. The human feature  $x_h$ , object feature  $x_o$ , and union region of both human and feature  $x_u$  obtained from the ResNet-101 FasterRCNN backbone are concatenated to form the joint relational visual features  $x_v$ . The semantic representation  $y_s$  is formed via a concatenation of the Glove [24] embedding of the human  $y_h$  and object  $y_o$ . We perform max pooling on the relational features,  $\mathcal{R}_i = r_1, r_2, \dots, r_n$  in a given snapshot,

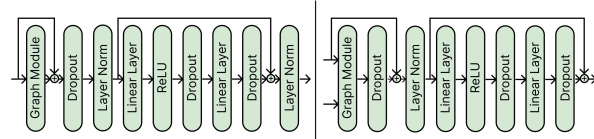


Figure 7: The graph neural network encoder (left) and graph neural network decoder (right) architecture. The residual connections are shown with the + sign. The graph module consists of equations 5-7 from the main paper.

where each  $r_k = [x_v, y_s]$  is the concatenation of visual and semantic features. Afterward, we pass these features into the 2-layer MLP. The inputs and outputs of the first layer are 1936 and 1936 dimensional respectively and we apply dropout with  $p = 0.5$ . The last layer is a classification layer and is made up of 1936 to 157 dimensional output to abduct actions. Lastly, we apply a sigmoid function before applying PyTorch’s multi-label margin loss to train the model.

## 6.7. GNNED: Relational Graph Neural Network Encoder-Decoder

The relational graph neural network encoder-decoder architecture we proposed is shown in Figure 7. The graph encoding layer (left) is very similar to the Transformer encoder layer [32]. The graph encoding layer consists of dropout layers, layer norm [2], linear layers, and residual connections [13]. The graph decoder layer (right) is also similar to a Transformer decoder layer except for the graph module.

## 6.8. GRU and Transformer decoder for abductive action sequence inference

We include the architecture design of the GRU and Transformer decoder used for action sequence prediction in Figure 8. We attached a 3-layer GRU decoder and a 2-layer Transformer decoder to our object-relational models for abductive action sequence inference. During training, we utilize a batch size of 1 video. We also freeze the weights of the FasterRCNN and object-relational models. To ensure

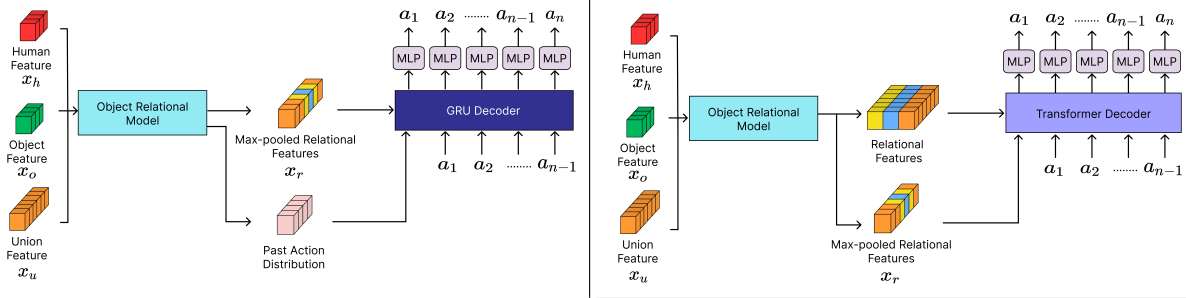


Figure 8: The GRU (left) and Transformer (right) decoder used in our main paper for the abductive action sequence inference task.

Model	Parameters
Relational MLP	13.4M
Relational Transformer	101.2M
Relational GNNED	80.7M
RBP	373.4M
BiGED	213.6M

Table 5: The object-relational model parameters for the abductive action inference task.

the sequence length matches across an entire batch, we pad each input sequence. We apply dropout of 0.1 and 0.5 for the GRU/Transformer decoder and MLP classifier respectively. As for the Transformer, we set the number of heads to 8. We trained both models using the element-wise cross-entropy loss. In addition, the output dimension of the MLP is set to 158 classes to account for a stop token. We refer the user to Table 6 for the number of parameters in the GRU and Transformer decoder.

### 6.9. Object-Relational Model Parameters

The parameters of our proposed object-relational models are shown in Table 5. The Rule-based Inference (RI) model does not have any parameters and is therefore omitted from the table. Based on the results from the main paper, we note that the Graph Neural Network Encoder Decoder (GNNED) model obtains better performance than the Transformer model even though it has lesser parameters. In addition, our proposed Bilinear Graph Encoder Decoder (BiGED) model has lesser parameters and performs comparable to or better than the Relational Bilinear pooling (RBP) model. These further demonstrate the effectiveness of the proposed GNNED, RBP, and BiGED models for the challenging task of abductive action inference.

### 6.10. Evaluation Metrics

Here, We outline the evaluation metrics used for the abductive action inference task. For the abductive action set

Sequence Models	Parameters
GRU	36.8M
Transformer	77.2M

Table 6: The action sequence decoder model parameters for the abductive action sequence inference task.

and verification sub-problems, we compute the mean Average Precision (mAP) across  $C = 157$  action classes:

$$mAP = \frac{1}{C} \sum_{i=1}^C AP_i \quad (16)$$

where  $AP$  is the average precision between the ground truth and inferred past actions based on the individual classes and for Recall@K ( $R@K$ ) across the test set  $N$ :

$$R@K = \frac{1}{N} \sum_{i=1}^N \frac{y_i \cap \hat{y}_i}{y_i} \quad (17)$$

where  $y_i$  and  $\hat{y}_i$  are the set of ground truth and inferred past actions for the  $i^{th}$  sample respectively. The mean Recall@K (mR@K) is computed per-class in a similar fashion to the Recall@K ( $R@K$ ) but instead we take the average over classes.

As for abductive action sequence prediction, we compute the element-wise accuracy between the ground truth and predictions by ignoring the padding, stop token and limiting the accuracy computation to the length of the ground truth actions.

### 6.11. Additional Quantitative Results

We provide a breakdown of the Recall@10 ( $R@10$ ) results for *Abduct at T* and *Abduct last snapshot* setups in Table 7 and Table 8 respectively for the abductive set inference task. The ability to abduct all past actions is important to real-life applications such as human-robot collaboration. In both setups,  $R@10$  for all models decreases as the number of actions in  $\mathcal{A}$  increases. This demonstrates that the

Model	$\mathcal{A}_1$	$\mathcal{A}_2$	$\mathcal{A}_3$	$\mathcal{A}_4$	$\mathcal{A}_5$	$\mathcal{A}_6$	$\mathcal{A}_7$	$\mathcal{A}_8$	$\mathcal{A}_9$	$\mathcal{A}_{10}$	$\mathcal{A}_{11}$	$\mathcal{A}_{12}$	$\mathcal{A}_{13}$	$\mathcal{A}_{14}$	$\mathcal{A}_{15}$	$\mathcal{A}_{16}$	$\mathcal{A}_{17}$	$\mathcal{A}_{18}$	$\mathcal{A}_{19}$	$\mathcal{A}_{20}$	$\mathcal{A}_{21}$	$\mathcal{A}_{22}$	$\mathcal{A}_{23}$	$\mathcal{A}_{24}$	$\mathcal{A}_{25}$	$\mathcal{A}_{26}$
RI	0.00	76.65	78.32	71.12	63.71	56.06	50.31	43.92	40.89	38.66	37.1	32.97	28.67	28.92	28.10	32.03	31.21	23.43	23.94	28.53	19.22	22.47	27.16	25.00	8.00	17.18
MLP	0.00	54.15	55.88	52.37	51.26	48.41	44.43	42.21	39.89	37.84	36.57	33.47	33.16	33.15	30.16	29.77	28.98	27.64	25.40	25.85	23.30	23.36	23.91	22.92	<b>16.80</b>	<b>21.54</b>
Transformer	0.00	74.29	74.43	70.39	66.99	62.94	57.61	54.19	50.25	48.04	46.40	42.63	41.45	40.35	39.04	37.86	35.17	33.57	33.14	32.31	34.24	29.55	32.17	28.47	10.40	19.74
GNNED	0.00	73.28	75.35	71.99	67.93	64.10	59.83	56.29	52.12	50.24	48.51	44.72	43.72	41.84	40.42	38.59	37.26	35.41	35.17	<b>35.97</b>	<b>37.13</b>	30.18	<b>34.23</b>	29.17	14.40	20.77
RBP	0.00	<b>77.35</b>	78.38	<b>75.19</b>	70.12	<b>67.08</b>	<b>62.75</b>	<b>59.09</b>	<b>54.85</b>	<b>52.78</b>	<b>51.10</b>	<b>46.85</b>	<b>46.39</b>	<b>43.65</b>	<b>42.12</b>	39.73	<b>38.35</b>	<b>36.19</b>	<b>36.63</b>	35.06	<b>37.59</b>	30.93	30.84	27.78	12.80	20.51
BiGED	0.00	74.69	<b>78.68</b>	74.71	<b>70.63</b>	66.66	62.42	58.80	54.55	52.28	50.05	45.94	45.24	43.41	41.08	<b>39.82</b>	36.69	36.12	35.10	34.83	36.96	<b>31.82</b>	33.57	<b>29.86</b>	14.40	17.95

Table 7: Breakdown of Recall@10 (R@10) results for all models on the abductive action set inference test set using the *Abduct at T* setup. For any  $\mathcal{A}_i$ ,  $\mathcal{A}$  denotes the action set and  $i$  is its cardinality.

Model	$\mathcal{A}_1$	$\mathcal{A}_2$	$\mathcal{A}_3$	$\mathcal{A}_4$	$\mathcal{A}_5$	$\mathcal{A}_6$	$\mathcal{A}_7$	$\mathcal{A}_8$	$\mathcal{A}_9$	$\mathcal{A}_{10}$	$\mathcal{A}_{11}$	$\mathcal{A}_{12}$	$\mathcal{A}_{13}$	$\mathcal{A}_{14}$	$\mathcal{A}_{15}$	$\mathcal{A}_{16}$	$\mathcal{A}_{17}$	$\mathcal{A}_{18}$	$\mathcal{A}_{19}$	$\mathcal{A}_{20}$	$\mathcal{A}_{21}$	$\mathcal{A}_{22}$	$\mathcal{A}_{23}$	$\mathcal{A}_{24}$	$\mathcal{A}_{25}$	$\mathcal{A}_{26}$
RI	0.00	61.90	67.74	59.54	58.93	51.53	46.73	44.04	41.03	39.24	37.93	35.14	32.02	31.99	34.03	34.05	32.18	25.15	24.21	25.62	34.52	<b>27.27</b>	31.52	25.00	19.23	
MLP	0.00	66.67	53.23	46.13	48.88	47.17	39.97	38.47	39.12	37.97	34.55	30.71	32.12	30.54	30.28	31.25	28.72	22.51	25.26	21.25	26.19	22.73	25.00	20.83	<b>23.08</b>	
Transformer	0.00	66.67	65.05	59.28	61.18	55.56	50.61	46.31	46.48	43.86	42.13	38.44	37.40	35.92	37.64	35.99	32.18	28.36	31.58	32.50	34.52	<b>27.27</b>	34.78	<b>29.17</b>	19.23	
GNNED	0.00	71.43	59.68	60.05	60.36	54.03	51.06	46.89	46.35	44.94	43.07	37.76	38.37	36.34	38.89	37.28	<b>33.56</b>	28.36	33.16	<b>34.38</b>	<b>35.71</b>	22.73	<b>35.87</b>	<b>29.17</b>	<b>23.08</b>	
RBP	0.00	<b>85.71</b>	<b>67.74</b>	61.86	62.01	<b>56.1</b>	53.50	48.25	47.93	<b>46.96</b>	44.14	38.29	38.27	37.16	<b>39.17</b>	<b>39.01</b>	33.22	29.53	<b>35.79</b>	33.13	33.33	<b>27.27</b>	31.52	25.00	<b>23.08</b>	
BiGED	0.00	<b>85.71</b>	61.29	<b>62.89</b>	<b>63.79</b>	55.99	<b>53.65</b>	<b>48.83</b>	<b>48.59</b>	46.65	<b>44.76</b>	<b>38.59</b>	<b>38.46</b>	<b>37.89</b>	38.33	36.64	30.80	<b>30.41</b>	35.26	33.13	32.14	<b>27.27</b>	<b>35.87</b>	<b>29.17</b>	19.23	

Table 8: Breakdown of Recall@10 (R@10) results for all models on the abductive action set inference test set using the *Abduct last snapshot* setup. For any  $\mathcal{A}_i$ ,  $\mathcal{A}$  denotes the action set and  $i$  is its cardinality.

task is indeed more challenging when we are abducting a large number of actions. Interestingly, all models obtained 0.00 R@10 when there is only a single action. We attribute the cause to the use of PyTorch’s multi-label margin loss which may not work for single label samples. Therefore, more research on choosing the appropriate loss function is required.

Based on the results, the proposed RBP and BiGED models obtain comparable and better performance across different length of past actions. An interesting observation can be made when we look at  $\mathcal{A}_{26}$  in both tables. Although the *Abduct last snapshot* setup is more difficult, the performance of R@10 is better than *Abduct at T* due to the fact that there is only a single snapshot in the  $\mathcal{A}_{26}$  action set for the *Abduct last snapshot* setup.

Apart from the two different setups mentioned in the main paper, we also provide additional results for a third setup. In the third setup, the action sets are formed from the current and previous snapshots which form the ground truth denoted by  $\mathcal{A} = \{\mathcal{A}_{t-1} \cup \mathcal{A}_t\}$ . We retrain all object-relational models with the corresponding past action set obtained from the current and previous snapshots. We report the results in Table 9. Similar trends to the previous tables in the main paper are observed here as well. The rule-based approach and MLP model perform the worse. Both GNNED and RBP outperform the Transformer model and BiGED is the best performer. Based on the results, we conclude that the GNNED, RBP models, and their combination (BiGED) are effective for abductive action inference. We also note the performance increase as it is an easier task as there are more snapshots that contain lesser amount of actions – see Figure 5.

## 6.12. Ablation Study

We perform ablation studies on our object-relational models. The two models used for the ablation studies are a 2-layer MLP and a Transformer. We use the setup where

Model	mAP	R@10	mR@10
Rule-based inference	26.06	56.65	45.55
MLP	30.46	59.62	41.68
Transformer	35.77	69.16	55.70
GNNED	36.00	69.13	56.91
RBP	36.07	71.48	56.67
BiGED	<b>37.45</b>	<b>71.84</b>	<b>57.95</b>

Table 9: Abductive action set inference performance using the proposed methods on the *Abduct from current and previous snapshots* setup.

Model	mAP	R@10	mR@10
MLP (visual only)	23.00	47.39	33.21
MLP (visual + scheduler)	22.87	46.98	32.54
MLP (visual + semantic)	30.44	<b>60.11</b>	<b>42.14</b>
MLP (visual + semantic + scheduler)	<b>30.46</b>	59.62	41.68
Transformer (visual only)	21.42	46.44	34.24
Transformer (visual + scheduler)	21.93	47.04	34.80
Transformer (visual + semantic)	35.40	68.47	54.90
Transformer (visual + semantic + scheduler)	<b>35.77</b>	<b>69.16</b>	<b>55.70</b>

Table 10: Ablation study for the impact of semantic features and scheduler on the abductive action set inference for the *Abduct from current and previous snapshot* setup.

Model	mAP	R@10	mR@10
MLP+mean pooling	28.49	58.01	40.12
MLP+max pooling	<b>30.46</b>	<b>59.62</b>	<b>41.68</b>
Transformer+mean pooling	35.31	68.93	54.55
Transformer+max pooling	<b>35.77</b>	<b>69.16</b>	<b>55.70</b>

Table 11: Ablation study for max pooling vs mean pooling for abductive action set inference *Abduct from current and previous snapshot* setup.

the model must abduct actions from the current and previous snapshots of the AG dataset. These findings can also be generalized to the other setups in the main paper.

**Impact of semantic features and learning scheduler.** We

evaluate the effect of visual and semantic (Glove [24]) features in Table 10. The use of semantic features provides a huge performance boost across all metrics. We attribute the performance increase to the contextual information provided by the semantics. The semantics of objects enables the model to identify and relate the actions effectively and provide an easier means to reason about actions. It is also interesting to see the impact of the learning rate scheduler which provides considerable improvement for the transformer model. Therefore, we use semantics and the learning rate scheduler for all our models.

**Max pooling vs Mean pooling.** We ablate the use of mean and max pooling on the relational features before feeding them into the classification layer to perform abductive action set inference – see Table 11. In the experiments, max pooling obtains better results for MLP and the Transformer model. Therefore, we utilize max pooling.

### 6.13. Additional Qualitative Results

We provide additional qualitative results on our object-relational models in Figure 9 for the abductive action set inference task. In the first snapshot, there are objects such as a person, floor, chair, dish, food, and box. In the second snapshot, there are objects such as a person, shelf, paper/notebook, book, and picture. In the third snapshot, there are objects such as a person, box, bed, and food. In the fourth snapshot, there are objects such as a person, sofa/couch, cup/glass/bottle, and chair. Here, we showcase examples that contain a huge set of past actions. In some cases, the rule-based model outperforms the MLP model and vice versa. Similarly, RBP and BiGED outperform the rest of the models.

Snapshot	Rule-based	MLP	Transformer	GNNED	RBP	BiGED
	Holding a dish Holding some food Holding a box Taking food from somewhere Someone is eating something Opening a box Sitting in a chair Sitting on the floor Putting some food somewhere Holding a cup/glass/bottle of something Taking something from a box	Holding a dish Holding some food Holding a box Taking food from somewhere Someone is eating something Opening a box Sitting in a chair Sitting on the floor Putting some food somewhere Holding a cup/glass/bottle of something Taking something from a box	Holding a dish Holding some food Holding a box Taking food from somewhere Someone is eating something Opening a box Sitting in a chair Sitting on the floor Putting some food somewhere Holding a cup/glass/bottle of something Taking something from a box	Holding a dish Holding some food Holding a box Taking food from somewhere Someone is eating something Opening a box Sitting in a chair Sitting on the floor Putting some food somewhere Holding a cup/glass/bottle of something Taking something from a box	Holding a dish Holding some food Holding a box Taking food from somewhere Someone is eating something Opening a box Sitting in a chair Sitting on the floor Putting some food somewhere Holding a cup/glass/bottle of something Taking something from a box	Holding a dish Holding some food Holding a box Taking food from somewhere Someone is eating something Opening a box Sitting in a chair Sitting on the floor Putting some food somewhere Holding a cup/glass/bottle of something Taking something from a box
	Holding a picture Putting their paper/notebook somewhere Taking paper/notebook from somewhere Holding a book Opening a book Putting a book somewhere Taking a book from somewhere Putting something on a shelf Watching/looking at a picture Reaching for and grabbing a picture Putting a picture somewhere Closing a door Closing a closet/cabinet Opening a closet/cabinet Holding some clothes somewhere Taking some clothes from somewhere Grasping onto a doorknob Someone is dressing	Holding a picture Putting their paper/notebook somewhere Taking paper/notebook from somewhere Holding a book Opening a book Putting a book somewhere Taking a book from somewhere Putting something on a shelf Watching/looking at a picture Reaching for and grabbing a picture Putting a picture somewhere Closing a door Closing a closet/cabinet Opening a closet/cabinet Holding some clothes somewhere Taking some clothes from somewhere Grasping onto a doorknob Someone is dressing	Holding a picture Putting their paper/notebook somewhere Taking paper/notebook from somewhere Holding a book Opening a book Putting a book somewhere Taking a book from somewhere Putting something on a shelf Watching/looking at a picture Reaching for and grabbing a picture Putting a picture somewhere Closing a door Closing a closet/cabinet Opening a closet/cabinet Holding some clothes somewhere Taking some clothes from somewhere Grasping onto a doorknob Someone is dressing	Holding a picture Putting their paper/notebook somewhere Taking paper/notebook from somewhere Holding a book Opening a book Putting a book somewhere Taking a book from somewhere Putting something on a shelf Watching/looking at a picture Reaching for and grabbing a picture Putting a picture somewhere Closing a door Closing a closet/cabinet Opening a closet/cabinet Holding some clothes somewhere Taking some clothes from somewhere Grasping onto a doorknob Someone is dressing	Holding a picture Putting their paper/notebook somewhere Taking paper/notebook from somewhere Holding a book Opening a book Putting a book somewhere Taking a book from somewhere Putting something on a shelf Watching/looking at a picture Reaching for and grabbing a picture Putting a picture somewhere Closing a door Closing a closet/cabinet Opening a closet/cabinet Holding some clothes somewhere Taking some clothes from somewhere Grasping onto a doorknob Someone is dressing	Holding a picture Putting their paper/notebook somewhere Taking paper/notebook from somewhere Holding a book Opening a book Putting a book somewhere Taking a book from somewhere Putting something on a shelf Watching/looking at a picture Reaching for and grabbing a picture Putting a picture somewhere Closing a door Closing a closet/cabinet Opening a closet/cabinet Holding some clothes somewhere Taking some clothes from somewhere Grasping onto a doorknob Someone is dressing
	Holding a box Taking a box from somewhere Opening a box Taking something from a box Holding some food somewhere Someone is eating something Taking food from somewhere Sitting in a bed Sitting on sofa/couch Watching television	Holding a box Taking a box from somewhere Opening a box Taking something from a box Holding some food somewhere Someone is eating something Taking food from somewhere Sitting in a bed Sitting on sofa/couch Watching television	Holding a box Taking a box from somewhere Opening a box Taking something from a box Holding some food somewhere Someone is eating something Taking food from somewhere Sitting in a bed Sitting on sofa/couch Watching television	Holding a box Taking a box from somewhere Opening a box Taking something from a box Holding some food somewhere Someone is eating something Taking food from somewhere Sitting in a bed Sitting on sofa/couch Watching television	Holding a box Taking a box from somewhere Opening a box Taking something from a box Holding some food somewhere Someone is eating something Taking food from somewhere Sitting in a bed Sitting on sofa/couch Watching television	Holding a box Taking a box from somewhere Opening a box Taking something from a box Holding some food somewhere Someone is eating something Taking food from somewhere Sitting in a bed Sitting on sofa/couch Watching television
	Sitting in a chair Drinking from a cup/glass/bottle Holding a cup/glass/bottle of something Taking a cup/glass/bottle from somewhere Putting a cup/glass/bottle somewhere Sitting on sofa/couch Watching television Sitting in a bed Someone is eating something	Sitting in a chair Drinking from a cup/glass/bottle Holding a cup/glass/bottle of something Taking a cup/glass/bottle from somewhere Putting a cup/glass/bottle somewhere Sitting on sofa/couch Watching television Sitting in a bed Someone is eating something	Sitting in a chair Drinking from a cup/glass/bottle Holding a cup/glass/bottle of something Taking a cup/glass/bottle from somewhere Putting a cup/glass/bottle somewhere Sitting on sofa/couch Watching television Sitting in a bed Someone is eating something	Sitting in a chair Drinking from a cup/glass/bottle Holding a cup/glass/bottle of something Taking a cup/glass/bottle from somewhere Putting a cup/glass/bottle somewhere Sitting on sofa/couch Watching television Sitting in a bed Someone is eating something	Sitting in a chair Drinking from a cup/glass/bottle Holding a cup/glass/bottle of something Taking a cup/glass/bottle from somewhere Putting a cup/glass/bottle somewhere Sitting on sofa/couch Watching television Sitting in a bed Someone is eating something	Sitting in a chair Drinking from a cup/glass/bottle Holding a cup/glass/bottle of something Taking a cup/glass/bottle from somewhere Putting a cup/glass/bottle somewhere Sitting on sofa/couch Watching television Sitting in a bed Someone is eating something

Figure 9: More qualitative results produced by each object-relational model on the abductive action set inference *Abduct last snapshot* setup on the AG test dataset. The first column shows the snapshot along with the object bounding boxes in the scene. The remaining columns show the actions predicted by each model. Actions highlighted in green are correctly inferred while the rest are ground truth actions that the model did not infer. The actions shown here are not in order, but for ease of comparison, we kept the ordering.